THE USE OF OPTICAL INTERFERENCE TO OBTAIN SELECTIVE ENERGY ABSORPTION

Douglas C. Martin and Ronald Bell
Spectrolab, Inc.

INTRODUCTION.

Solar radiation offers a virtually inexhaustible source of energy. With foreseeable depletion of the earth's store of fossil fuel and the recognized need for auxiliary power for space vehicles, there is an increasing interest in efficient solar energy conversion. Except for very short missions, all space flights to date have been powered by direct photovoltaic quantum conversion of solar energy using silicon solar cells. Several other conversion systems are under investigation and some have been in varying degrees reduced to practice. Most of these systems, e.g. thermoelectric, thermionic and solar turbine, are dependent upon the thermodynamic conversion of energy from a source heated by absorption of solar irradiance. Fundamental to the effiency of these systems is a receiver having high absorption in the spectral range from about 0.3μ to 1.5μ, which includes about 90% of the solar energy, and low radiation loss over the range of operating temperatures.

The theoretical maximum efficiency of a heat-work transformation is governed by the thermodynamic equation: $\eta = (T_1-T_2)/T_1$ where T_1 is the temperature in degrees K of the heat source and T_2 is that of the heat sink. In practice, this efficiency is never achieved because of system losses arising from non-useful work, re-radiation into space, low electrical conversion factors, etc. Nevertheless, the maximum fraction of the incident solar energy that may be converted to useful work is dependent upon the temperature difference $T_1 - T_2$. By careful design, very low heat sink temperatures can generally be achieved. The challenge is in development of high source temperatures in stable materials. The most direct method for producing the high temperatures is by use of solar flux concentrators with ratios of 100 to 1 and higher. However, the successful deployment of a high-ratio concentrator necessitates large area arrays, high optical precision and close orientation with respect to the radiation source.

The difficulties associated with these requirements are so significant that every effort is being made to reduce the concentration ratios. For a specified energy utilization at a given ultimate source temperature, the minimum concentration ratio will be required for a source having the highest absorption of solar energy and the smallest non-useful losses by radiation, conduction, etc. This paper describes a method for surface

treatment directed toward optimization of these properties for auxiliary power systems of space vehicles.

THERMAL BALANCE

The heat input to an object in space is the summation of absorbed solar energy, albedo and thermal energy from planets and nearby auxiliary (vehicle) surfaces, internal power losses, and conduction from other portions of the vehicle. The energy output is the summation of thermal radiation to space and nearby surfaces, conduction to other portions of the vehicle, and converted electrical energy. The equilibrium temperature is that at which the sum of energy input and output is equal to zero, i.e., $Q_I + Q_O = 0$.

If there is sufficient isolation that all secondary factors, such as albedo, conduction, etc., can be neglected, then the thermal balance equation can be written with simply three terms:

(a) (b)

$$\int_{A_F}\int_{\lambda}\alpha(\lambda,\vec{r},\hat{E}\cdot\hat{n})\left[\vec{E}(\lambda)\cdot\hat{n}\right]dA\,d\lambda - \int_{A_R,A_F}\int_{\lambda}\alpha(\lambda,\vec{r})\,\frac{a\lambda^{-5}}{e^{b/\lambda T_i}-1}\,dA\,d\lambda$$

(1c)

$$-\int_{A_R,A_F}\int_{\lambda}\eta(T_1,T_2,\vec{r})\left[\vec{E}(\lambda)\cdot\hat{n}\right]dA\,d\lambda = 0$$

(Equation 1)

Where:
- A_F = Area of front of component
- A_R = Area of rear of component
- r = position vector
- n = unit vector normal to surface at endpoint of the appropriate position vector
- η = electrical conversion efficiency
- α = spectral absorptivity
- T_1 = temperature of heat source, ^{o}K
- T_2 = temperature of heat sink, ^{o}K
- a,b = coefficients, Planck's black body radiation equation
- E = solar irradiance

Defining the effective solar absorptivity, thermal emissivity and conversion efficiency, respectively, as:

$$\bar{\alpha} = \frac{\int_{A_F}\int_{\lambda}\alpha\vec{E}\cdot\hat{n}\,dA\,d\lambda}{\int_{A_F}\int_{\lambda}\vec{E}\cdot\hat{n}\,dA\,d\lambda}$$

(Equation 2)

$$\bar{\varepsilon}_F = \frac{\int_{A_F}\int_{\lambda} \frac{\alpha a \lambda^{-5}}{e^{b/\lambda T_1} - 1}\, dA\, d\lambda}{A_F \int_{\lambda} \frac{\alpha \lambda^{-5}}{e^{b/\lambda T_1} - 1}\, dA\, d\lambda} \qquad \text{(Equation 3a)}$$

$$\bar{\varepsilon}_R = \frac{\int_{A_R}\int_{\lambda} \frac{\alpha a \lambda^{-5}}{e^{b/\lambda T_1} - 1}\, dA\, d\lambda}{A_R \int_{\lambda} \frac{\alpha \lambda^{-5}}{e^{b/\lambda T_1} - 1}\, dA\, d\lambda} \qquad \text{(Equation 3b)}$$

$$\bar{\eta} = \frac{\int_{A_F}\int_{\lambda} \eta \vec{E} \cdot \hat{n}\, dA\, d\lambda}{\int_{A_F}\int_{\lambda} \vec{E} \cdot \hat{n}\, dA\, d\lambda} \qquad \text{(Equation 4)}$$

The radiative term, 1b, can then be written in terms of the more familiar Stefan-Boltzman law, and for an oriented map the thermal balance equation simplifies to:

$$(\bar{\alpha} - \bar{\eta})E - (\bar{\varepsilon}_R + \bar{\varepsilon}_F)\sigma T_1^4 = 0 \qquad \text{(Equation 5)}$$

where σ is the Stefan-Boltzman constant = 5.67×10^{-12} watts/cm^2/degree K^4. ε = Emissivity

Solving this implicit equation for T_1 (note that both N and E are functions of T)

$$T_1 = \sqrt[4]{\frac{(\bar{\alpha} - \bar{\eta})E}{(\bar{\varepsilon}_R + \bar{\varepsilon}_F)\sigma}} \qquad \text{(Equation 6)}$$

A plot of T_1 vs. insolance, E, is shown in Figure 1 for different values of the value $(\bar{\alpha} - \bar{\eta}) / \bar{\varepsilon}_R + \bar{\varepsilon}_F$.

OPTICALLY ENHANCED SELECTIVE MIRRORS

In 1956, Haas, Schoreder and Turner reported (JOSA, Jan 1956) a "dark

mirror" for application in reducing stray light in infrared instruments. A multiple film system was used to "antireflect" an aluminum mirror over the visible and near infrared. The longer wave reflection was not appreciably affected. The interesting spectral selectivity of these coatings suggest their application, with certain modifications, to the problem posed in this paper.

In Figure 2 are shown the solar spectral distribution, the spectral absorptivity of a dark mirror coating, and the product of these two distributions (representing the spectral distribution of absorbed solar energy). The effective solar absorptivity, computed according to equation 2 above, is 86%. Thus, for an air-mass-zero insolance of 1400 watts/m^2, about 1200 watts of energy are absorbed.

Referring again to Figure 2, the coating is seen to exhibit a sharp drop in absorptivity beyond about 1.4 μ to about 4% at 4 μ . A solution of Equation 6 (for $\eta = 0$) results in an equilibrium temperature of about 370°C for an isolated panel coated on both sides with the "dark mirror" illuminated by one sun. If the rear surface were freshly evaporated gold ($\bar{\varepsilon}$ =.025) then the panel temperature would be about 420°C.

Figure 3 shows the spectral reflectance for newly evaporated gold, copper, and aluminum. It will be noted that gold and copper inherently are excellent wave discriminators, being superior reflectors in the infrared and reasonably good absorbers of the short-wave solar irradiance. A polished gold plate actually has a calculated α/ε above 10. An isolated gold panel would reach an equilibrium temperature of about 320°C at normal solar incidence near Earth. Thus, a simple gold film would be almost as effective as the more complex dark mirror for a passive thermal balance system. But for an active conversion application, the much lower absorptivity of gold, about 0.25 compared to at least .86 for a dark mirror, would be a significant disadvantage. Moreover, for the desired very high temperatures, other metals have superior environmental characteristics compared to gold. However, they also have appreciably lower solar absorptivities and higher thermal emissivities. The problem then may be presented as the twofold approach of improving environmental stability for gold and modification of surface characteristics of both gold and other metals so as to increase the shortwave absorbance and at the same time not reducing and, if possible, even increasing the inherently low emissivity. A very effective method for accomplishing this is through application of one or more thin films which antireflect the metal by matching its optical impedance, using interference.

The reflectance reduction of suitable metals can be simply achieved by the deposition of an effectively one-quarter-wave-thick dielectric layer, although, as is shown later, not as completely as through the application of several interference films. In theory, the reflectance of any metal, including those whose uncoated reflectance is high, can be significantly reduced by a single $\lambda/4$ thick layer. If the effectively $\lambda/4$ thick layer is made sufficiently absorbing that the intensity of light reflected from the metal-dielectric interface falls off to a value matching the initial reflectance of the outer dielectric surface, near zero reflectance can be

expected at λ. Figure 4 shows the effect of single absorbing and non-absorbing layers on aluminum.

In Figure 5 the spectral reflectance of the Haas, et al "dark mirror" demonstrates how a three layer "antireflecting" system can increase the solar absorptivity without significantly affecting the low thermal (infrared) emissivity.

DARK MIRROR DESIGN

The mathematical treatment of multilayer interference systems can be approached from two opposite directions:

a. The synthesis of layer arrangements to match the required spectral characteristics.

b. Analysis of configurations which have been selected on the basis of past experience, and the application of a refining process based on Taylor's series to produce by successive approximation the matching of the required spectral characteristics.

In general the analytical techniques are highly suitable for the study of the properties of any given configuration. The synthesis method is most difficult even for a few layers, and for large numbers of layers is virtually beyond the capacity of modern computers. Moreover, system constraints must be imposed to restrict the materials to realizable media. Actually an effective compromise between synthesis and analysis represents the best system design approach. The two basic methods will be discussed briefly below:

a. Synthesis Method

The techniques discussed in this section permit the required optical properties of the individual layers to be determined from the given properties of the multilayer system. It can be shown that synthesis methods would be exceptionally complicated, and in many cases practically insoluble, if they were formulated generally. It is therefore necessary to consider the limited cases that are soluble. In one approach, the refractive indexes of the films can be specified and the required properties are obtained by selection of film thickness. Alternatively, one can proceed in the reverse direction, specifying the film thickness and determining the refractive indexes required. If the second system is chosen, i.e., the optical thicknesses are given, the functions for the intensity of reflected or transmitted light lead to curves which are extremely amenable to analysis. If the required value of the transmissivity, τ, is written as a function of cos $x/2$ or sin $x/2$, where x is the phase difference of the light rays in any given film, the following symmetrical polynomials are obtained.

$$\frac{1}{T} = A_{K_0} + A_{K_2}\Lambda^2 + A_{K_4}\Lambda^4 + \cdots + A_{K_{2K}}\Lambda^{2K}$$

$$= B_{K_0} + B_{K_2}\Lambda_1^2 + B_{K_4}\Lambda_1^4 + \cdots + B_{K_{2K}}\Lambda_1^{2K} \quad \text{(Equation 7)}$$

where $\Lambda = \cos x/2$ and $\Lambda_1 = \sin x/2$, and when the optical paths in all films are equal, i.e., $\bar{x} = 2\,n_1d_1 = 2\,n_2d_2 = \cdots\cdots = 2\,n_kd_k$.

The coefficients A and B are combinations of refractive indexes of the different films and those of the adjacent media; air, n_o, and substrate n. The solution of such polynomials can be obtained by matrix calculus and the results are given by Pohlock[1]. In practice, it is usually required of a system of films that its transmissivity or reflectivity in the limits of required spectral band be kept within the given values τ_m and τ_e. A general configuration of the curve given by Equation 6 shows that optimum use of the available parameters occurs if the polynomial of the nth degree has n - 1 extreme values, and these extremes alternately reach the limiting values of the prescribed function. In equation 6is shown a polynomial of the 6th degree which corresponds to a configuration of three thin films having identical optical thickness. To obtain clear expressions which relate the properties of the given data with the optical parameters, it is necessary to introduce the auxiliary polynomial $P(\Lambda/\Lambda_\omega)$.

This auxiliary polynomial is required to have the same form of oscillation between $P = -1$ and $P = +1$ in the interval $-1 \leq \Lambda/\Lambda_\omega \leq +1$ as in the specified function $1/\tau$ between the value $1/\tau_m$ and $1/\tau_e$ in the spectral region $-\Lambda_\omega \leq \Lambda \leq +\Lambda_\omega$.

Functions meeting this requirement are Tschebyscheff polynomials of the first order. In the consideration of a 3 film combination, the required function is of the 6th degree as given below:

$$P_6 = -1 + 18(\Lambda/\Lambda_\omega)^2 - 48(\Lambda/\Lambda_\omega)^4 + 32(\Lambda/\Lambda_\omega)^6, \quad \text{(Equation 8)}$$

which gives an intensity function of 3 films in the form of

$$\frac{1}{T} = P_6\left[\tfrac{1}{2}(1/\tau_e - 1/\tau_m)\right] - \tfrac{1}{2}(1/\tau_e + 1/\tau_m)$$

$$= \frac{1}{\tau_m} + 9\frac{(1/\tau_e - 1/\tau_m)}{\Lambda_\omega^2}\Lambda^2 - 24\frac{(1/\tau_e - 1/\tau_m)}{\Lambda_\omega^4}\Lambda^4 + 16\frac{(1/\tau_e - 1/\tau_m)}{\Lambda_\omega^6}\Lambda^6 \quad \text{(Equation 9)}$$

[1] Jenair Jahrbuch 1952 P. 181-221

A comparison of the coefficients of this equation with Equation 7 gives a series of equations below for the 3 film case:

$$A_{30} = 1/T_m \; ; \; A_{32} = \frac{9(1/T_e - 1/T_m)}{\lambda_w^2} \qquad \text{(Equations 10)}$$

$$A_{34} = \frac{-24(1/T_e - 1/T_m)}{\lambda_w^4} \; ; \; A_{36} = \frac{16(1/T_e - 1/T_m)}{\lambda_w^6}$$

from which the required refractive indices n_1, n_2 and n_3 can be derived from tables and curves given in References 1 and 2. In practice it may be found that the optimum polynomial cannot be realized because of the limited range of optical properties available in practical materials. It is then necessary to consider a polynomial of a lower order.

b. Analytical Method

The basic design of dark mirrors considered is based on the concept of anti-reflecting metal mirrors in the region of maximum solar energy with a series of dielectric and absorbing films while maintaining or even enhancing reflection in the long wavelength thermal region. In general, the number of thin films used is relatively small, thus allowing analysis of the reflectivity vs. to be performed manually by the use of Rouard's method which can be schematically written as follows:

$r_{(k+1)}$ $\qquad$ $r_k e^{i\bar{\delta}_k}$

$r_{(k)}$ $\qquad$ $r_{(k-1)} e^{i\bar{\delta}_{(k-1)}}$

$r_{(k-1)}$

$\cdot$ $\qquad$ $\vdots$

$\cdot$

$\cdot$

r_3

r_2 $\qquad$ $r_2 e^{i\bar{\delta}_2}$ $\qquad$ $r_1 e^{i\bar{\delta}_1} - r e^{i\bar{\delta}}$

r_1

where r is the Fresnel coefficient

---

2 Optics 3 1952 P. 498 Schroeder H.

$$\text{and } r_k e^{i\bar{\delta}_k} = \frac{r_k + r(k+1)e^{-ix_k}}{1 + r_k\, r(k+1)e^{-ix_k}}$$

where the phase difference is $x =$, where n is the refractive index of the film and d its physical thickness. Various configurations of possible dark mirrors have been considered and evaluated by means of these techniques and the results are shown in Figures 7 to 12. It will be noted that very close agreement is obtained with measured values for SiO, Al, SiO on an opaque substrate of aluminum as shown in Figure 5.

MATERIAL SELECTION

The original Haas et al "dark mirror" was constructed around an evaporated opaque aluminum film. Application of this system to the solar conversion receiver of an auxiliary power system, is unsatisfactory because of the relatively low melting point of aluminum (660°C) and its high chemical activity. Moreover, its high reflectivity over the entire solar spectrum complicates the antireflection problem.

In addition to having the required optical properties, materials used in practical receiver configurations must also have satisfactory mechanical and chemical properties at high temperatures in the space environment. It is desirable to choose for the substrate and (when required) for the absorbing film, metals which have both low volatilities and low electrochemical potentials. In this way, confidence can be gained that evaporation, diffusion and chemical reactions will be small. Of course, it is also essential that the metal substrate have high infrared reflectivity, particularly in the region of 2 to 5 μ.

In Table I is a partial list of metallic elements with melting points greater than 1100°K, whose evaporation into free space would be less than 10m of thickness per year, and which do not have other obviously disqualifying characteristics. In the table are shown the thicknesses evaporated (into free space) in one year, the electro-positive potentials, and typical reflectances at 4 μ. Materials which are electro-positive are likely choices for the dielectric cation, and metals with good infrared reflectance and low electrochemical potentials are recommended for the substrates and absorbing films.

For the dielectric materials the operating temperatures clearly preclude all salts except oxides and possibly a limited number of oxyfluorides (mainly of the rare earths). Even the rare earth fluorides have excessive volatilizations. Calcium fluoride, the most stable fluoride, losses 2×10^{-4} mm/yr and moreover is hygroscopic. In order to reduce the possibility of chemical reaction with the adjacent layers, the dielectric cations should have higher electrochemical potentials than the adjacent metals. By selecting the lowest possible cation valence combinations, disproportionation can be minimized, but individual reactionsshould never-

theless be separately considered.

The relevant properties of some stable oxides are shown in Table II. In addition to the oxides of metals included in Table I, it is seen that a few others have satisfactory binding energies. The refractive index ranges from 1.48 to 2.16, with a good selection around 1.9.

To be sure, some of the materials mentioned in the above description are not readily evaporated by conventional means. Since high optical surface quality and specularity are not essential to the application, other deposition techniques than high vacuum evaporation should be considered. Some of the listed materials can be plated, some can be mechanically worked, some can be sputtered and others can be chemically deposited. The feasibility of producing stable spectrally selective receivers utilizing optical interference techniques is theoretically possible, and for many configurations their fabrication is well within the present state-of-the-art. Current investigations demonstrate progress toward the ultimate goal of a stable receiver absorption coating for use in a space auxiliary power system.

SELECTED PROPERTIES OF STABLE METALS

TABLE I

Element	Thickness (mm) Vaporized Per Year Into Vacuum at 1000° K M (Solid) --- M(g*)	Electro-Chemical Potential	Reflectance (ρ) at $\lambda=4\mu$
Cobalt	10^{-5}	+0.227	81
Iridium	10^{-15}	(-)	94
Iron	10^{-5}	+0.44	89
Molybdenum	10^{-17}	+0.2	90
Nickel	10^{-5}	+0.250	92
Palladium	10^{-5}	-0.987	88
Platinum	10^{-12}	-1.2	91.5
Rhodium	10^{-12}	-0.8	92
Tantalum	10^{-24}	E+ at high temp.	93
Titanium	10^{-8}	+1.63	
Tungsten	10^{-27}	low	93
Vanadium	10^{-10}	+1.18	79
(Gold)	$>10^{-5}$	-1.42	98

* Ideal monatomic gas (does not include secondary transitions)

SELECTED PROPERTIES OF STABLE OXIDES

TABLE II

Oxide	Thickness (ma) Vaporized Per Year Into Vacuum at 1000°K M (Solid)----M (g*)	Cation Electro-Chemical Potential	Refractive Index of Bulk Material**
Al_2O_3	10^{-12}	1.66	1.76
BaO	10^{-6}	2.9	---
BeO	10^{-13}	1.85	1.72
CaO	10^{-11}	2.87	1.84
FeO	10^{-8}	.44	---
MgO	10^{-9}	2.37	1.74
MnO	10^{-8}	1.18	2.16
SiO_2	10^{-7}	---	1.48
SrO	10^{-9}	2.89	---
Ta_2O_5	10^{-5}	---	---
TiO	10^{-7}	1.63	---
ZrO_2	10^{-11}	1.53	2.15

* Ideal gas (does not include secondary transitions)

** Indexes of films will vary, but will not differ greatly from those of bulk materials

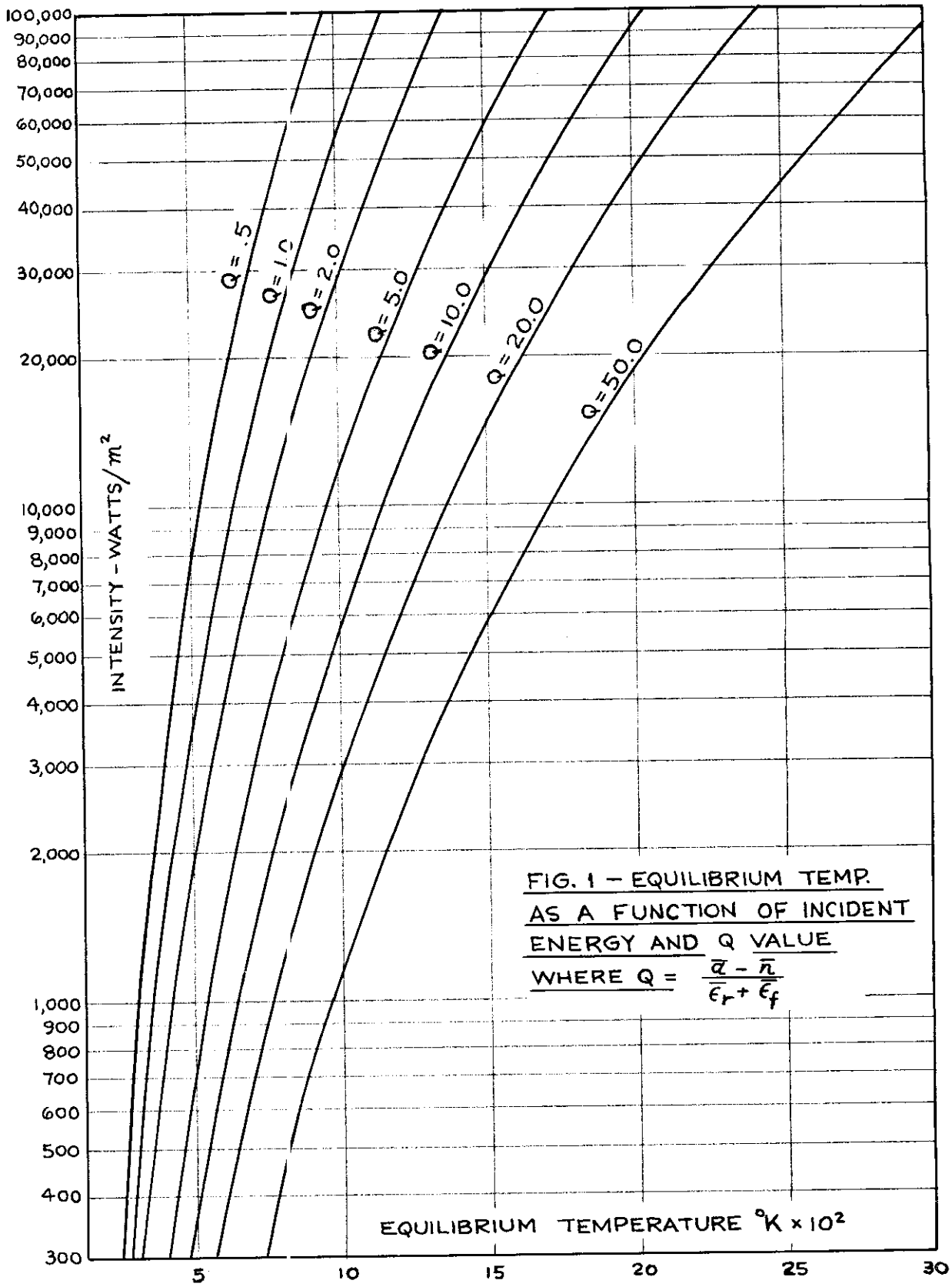

FIG. 1 – EQUILIBRIUM TEMP. AS A FUNCTION OF INCIDENT ENERGY AND Q VALUE WHERE $Q = \frac{\bar{a} - \bar{n}}{\bar{\epsilon}_r + \bar{\epsilon}_f}$

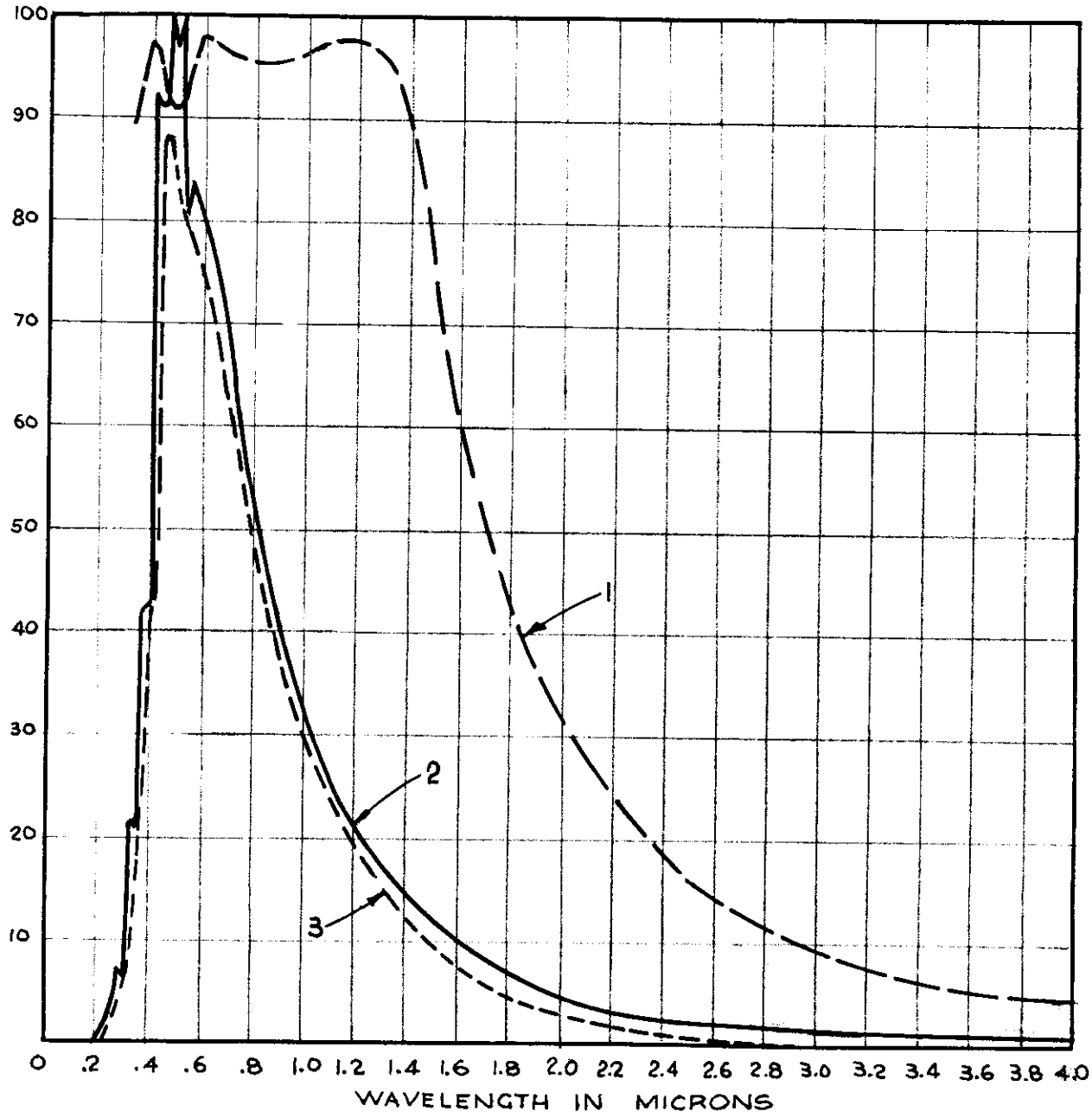

Figure 2 (1) Spectral Absorbance of Typical "Dark Mirror"
(2) Zero-air-mass Solar Energy Distribution
(3) Product of Curves (1) and (2)

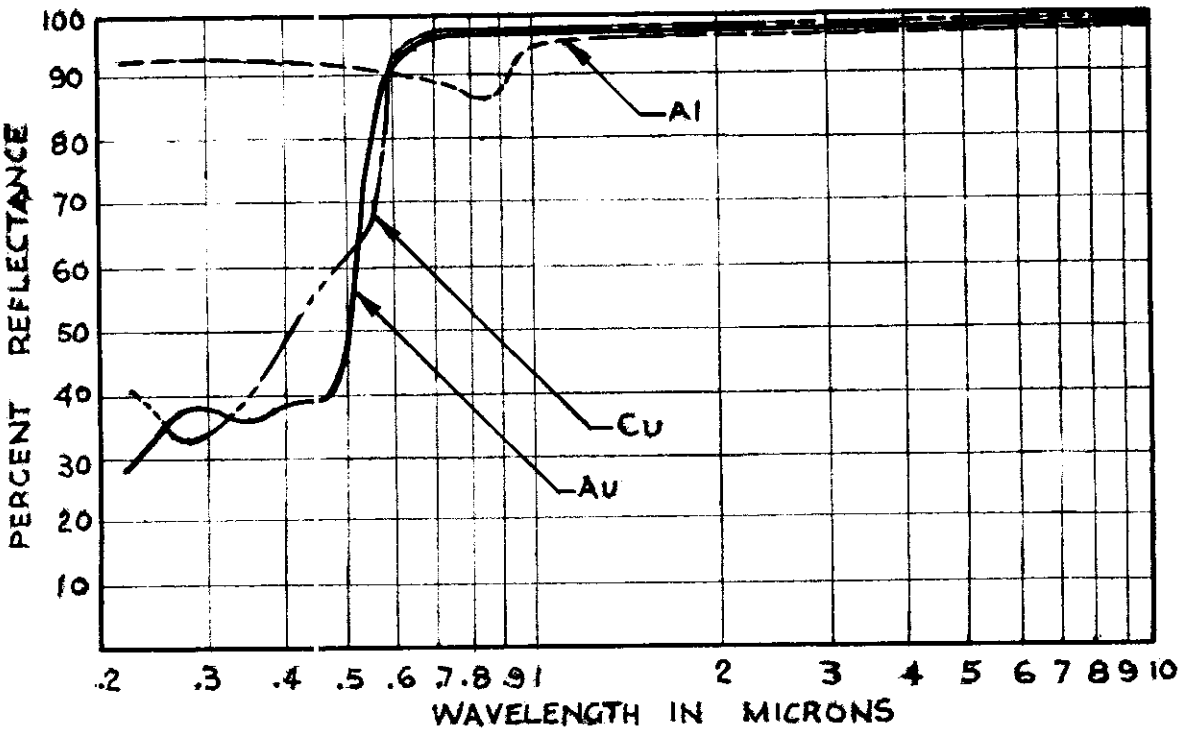

Figure 3 Spectral Reflectance of Evaporated Aluminum, Copper and Gold (Hass, et al, JOSA January 1956).

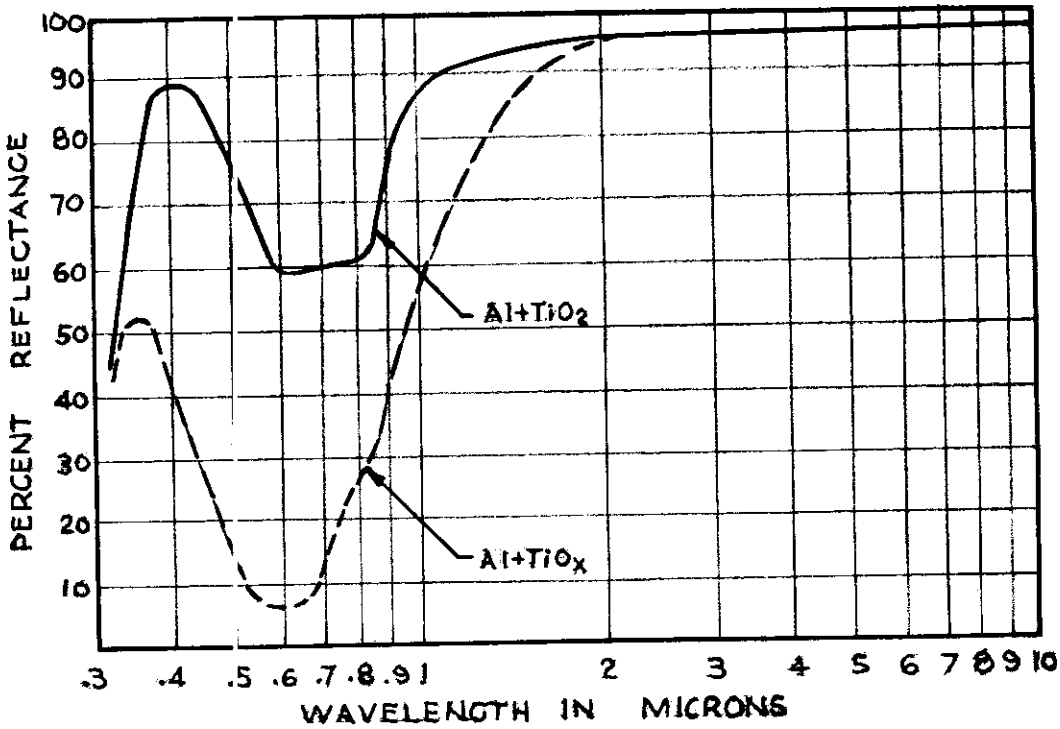

Figure 4 Spectral Reflectance of Aluminum Overcoated with Nonabsorbing Dielectric (TiO_2) and absorbing Dielectric (TiO_x) (Ref. Hass, et al, JOSA January 1956)

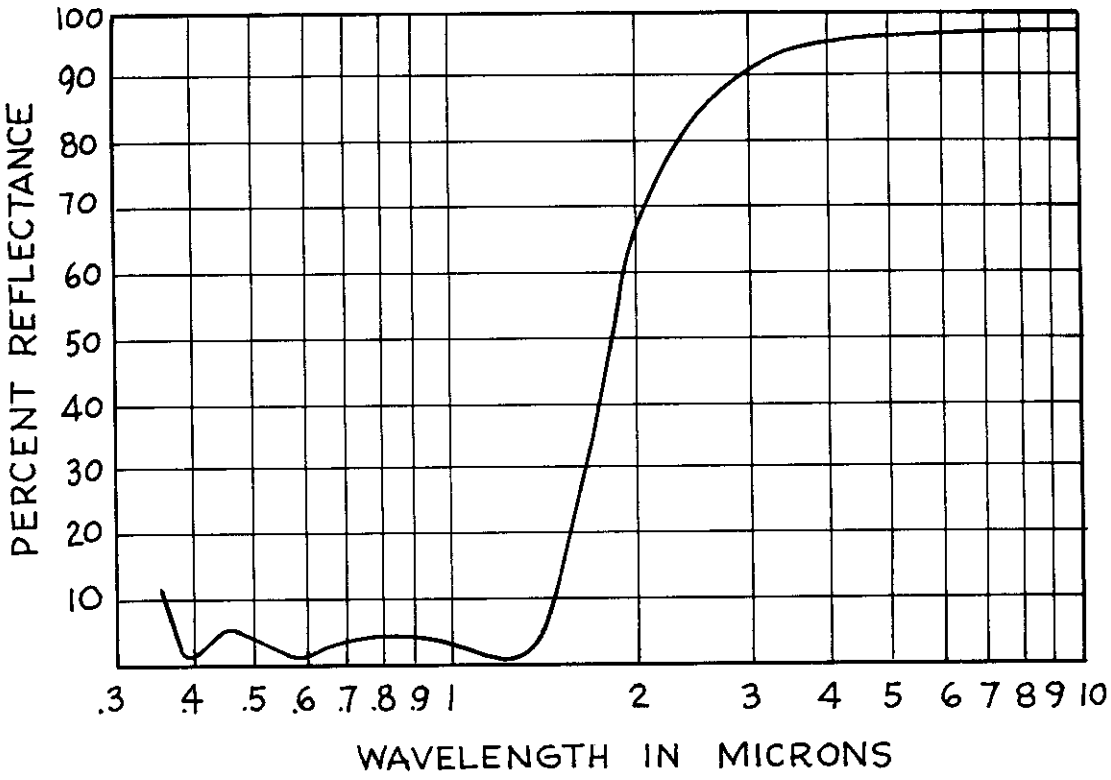

FIG. 5 - REFLECTANCE OF HASS, ET. AL. MIRROR (JOSA JAN. 1956)

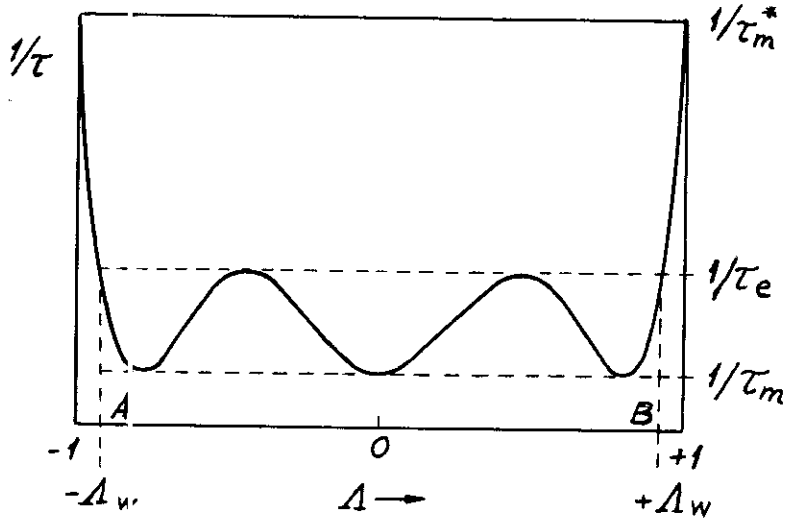

Figure 6 Graphic Representation of Polynomial of 6th Degree with 5 Prescribed Extreme Values

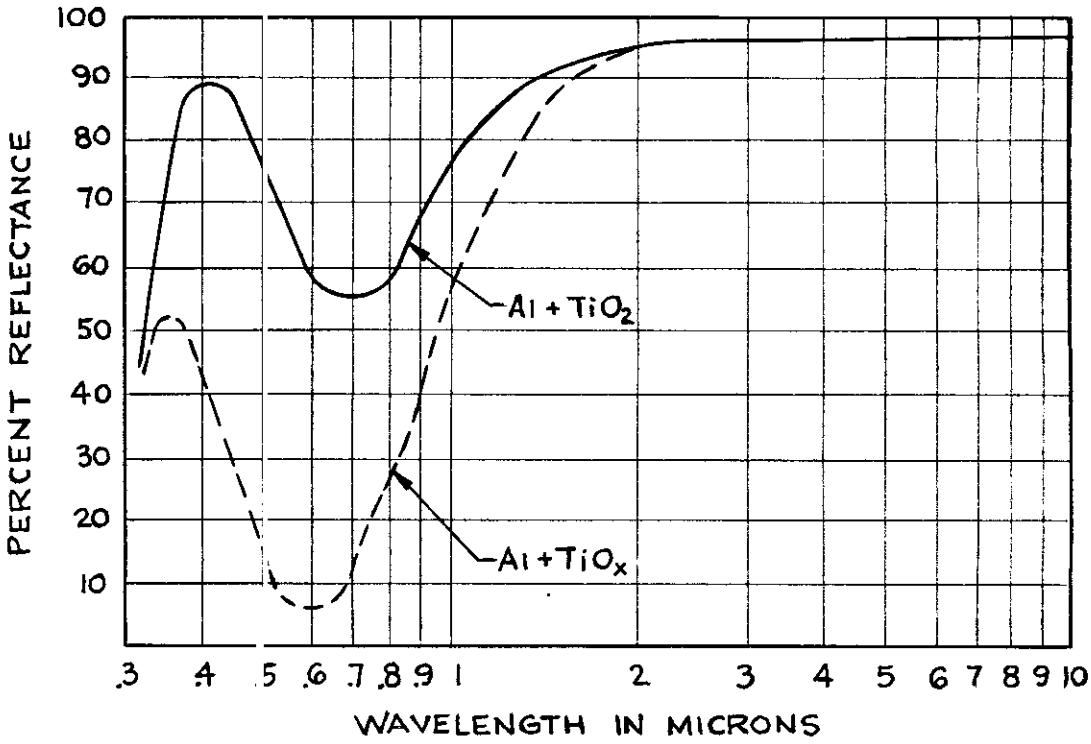

Figure 7 Theoretical Reflectance Curve For Al + TiO_2 & Al + $\frac{1}{2}(TiO_2 + TiO)$

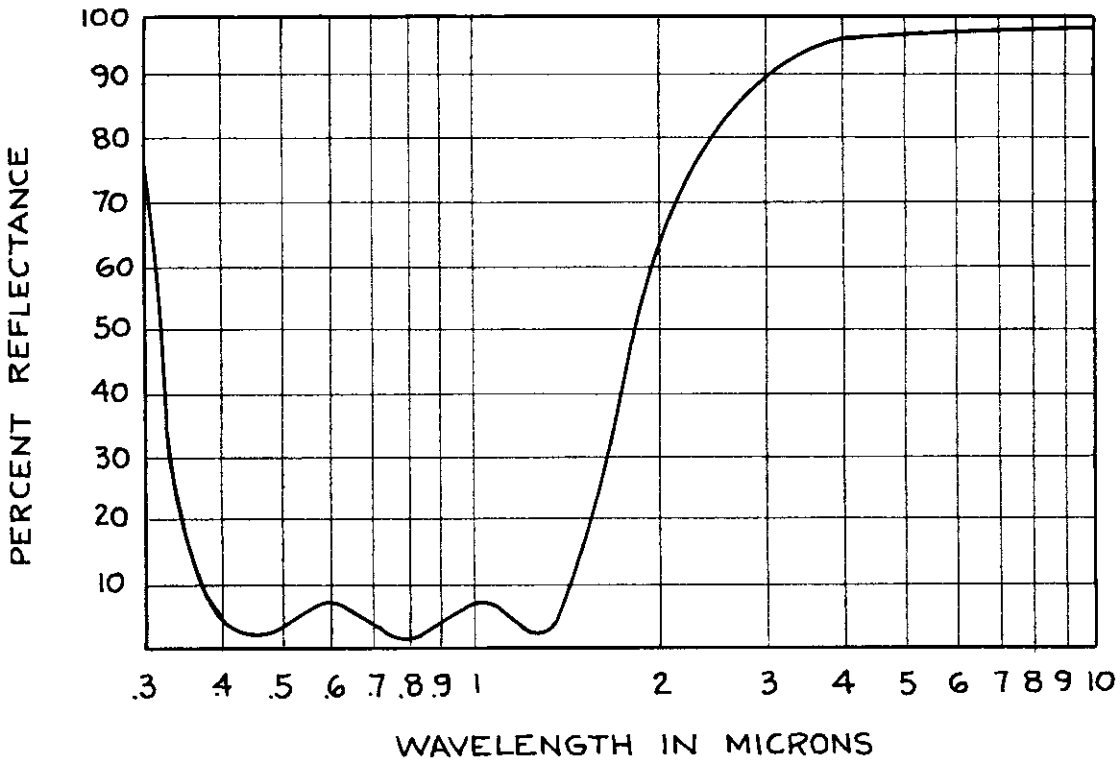

Figure 8 Theoretical Reflectivity of AL-SiO_2-AL-SiO_2

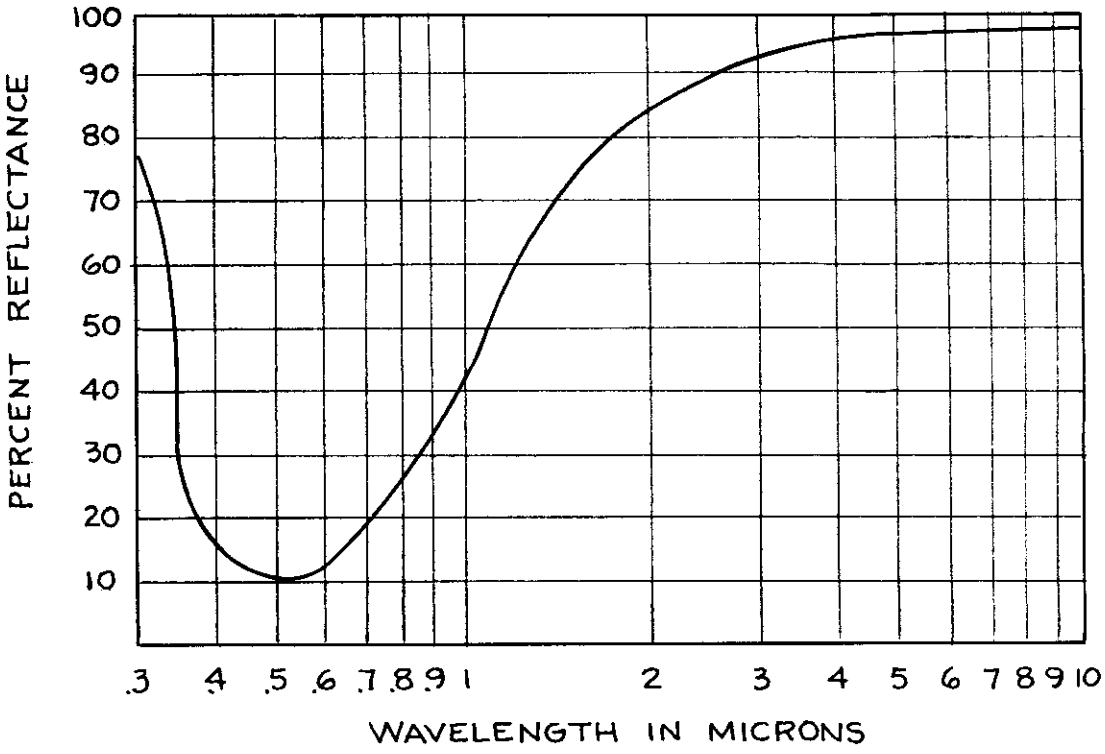

Figure 9 Theoretical Reflectivity of Anti-Reflected With SiO_2 Gold Film

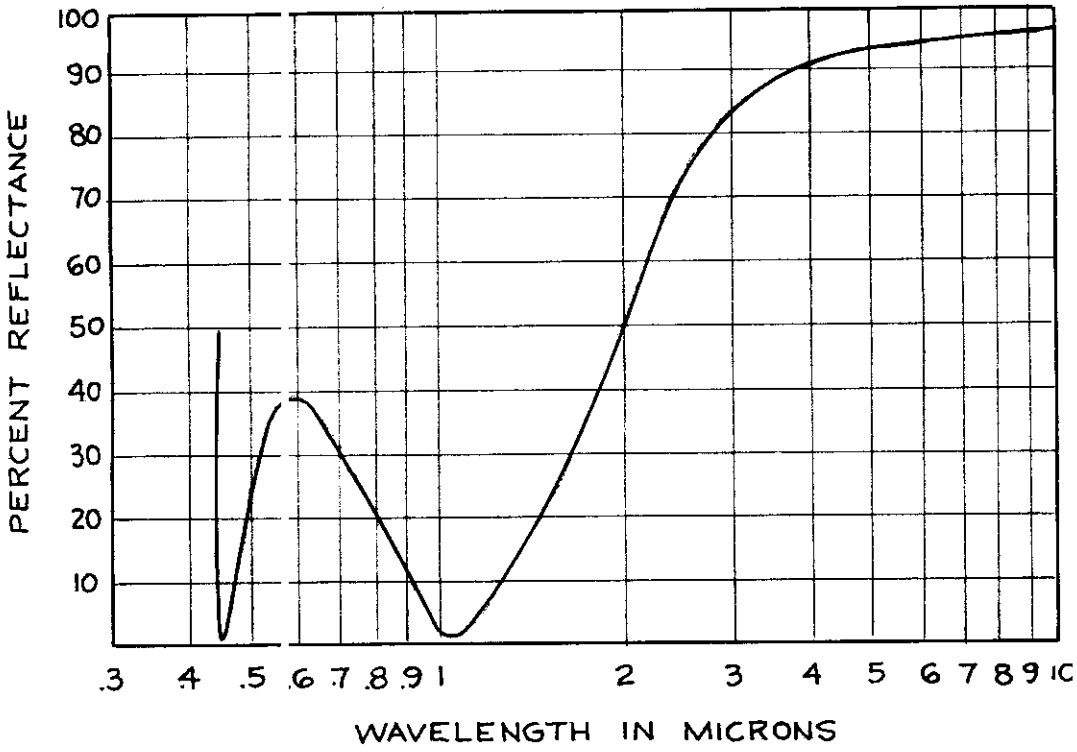

Figure 10 Theoretical Reflectivity of AL-TiO_2-AL-TiO_2

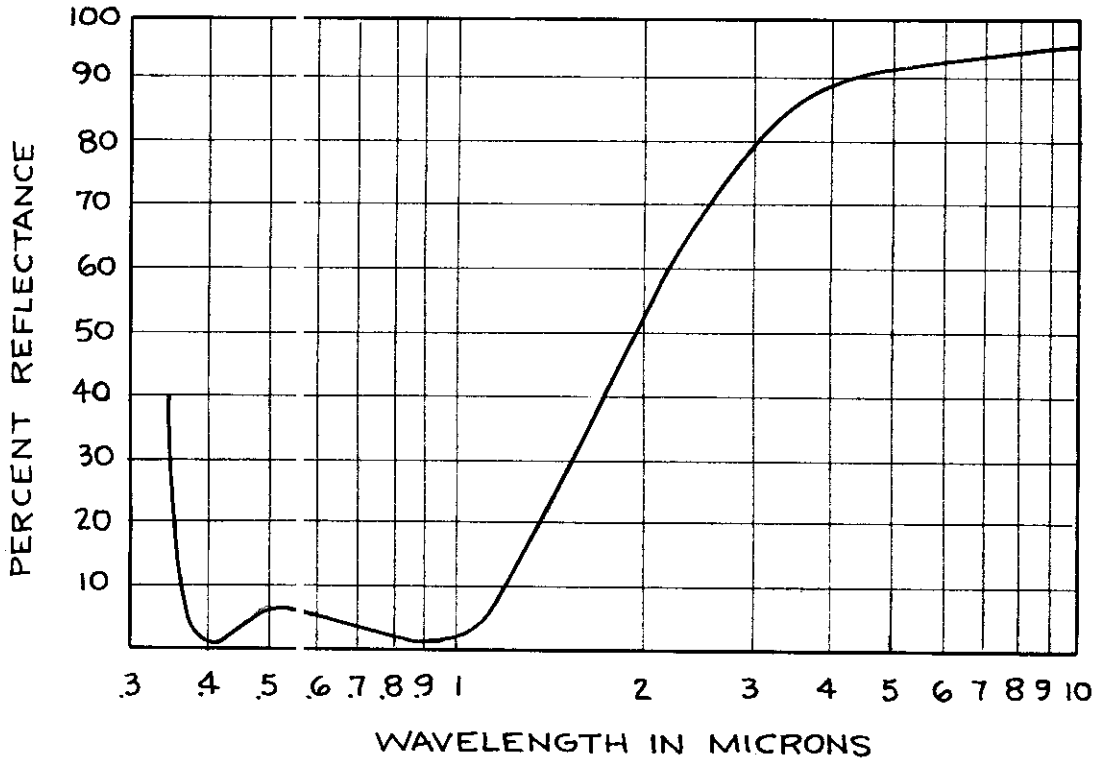

Figure 11 Theoretical Reflectivity of AL-SiO_2-Inconel-SiO_2

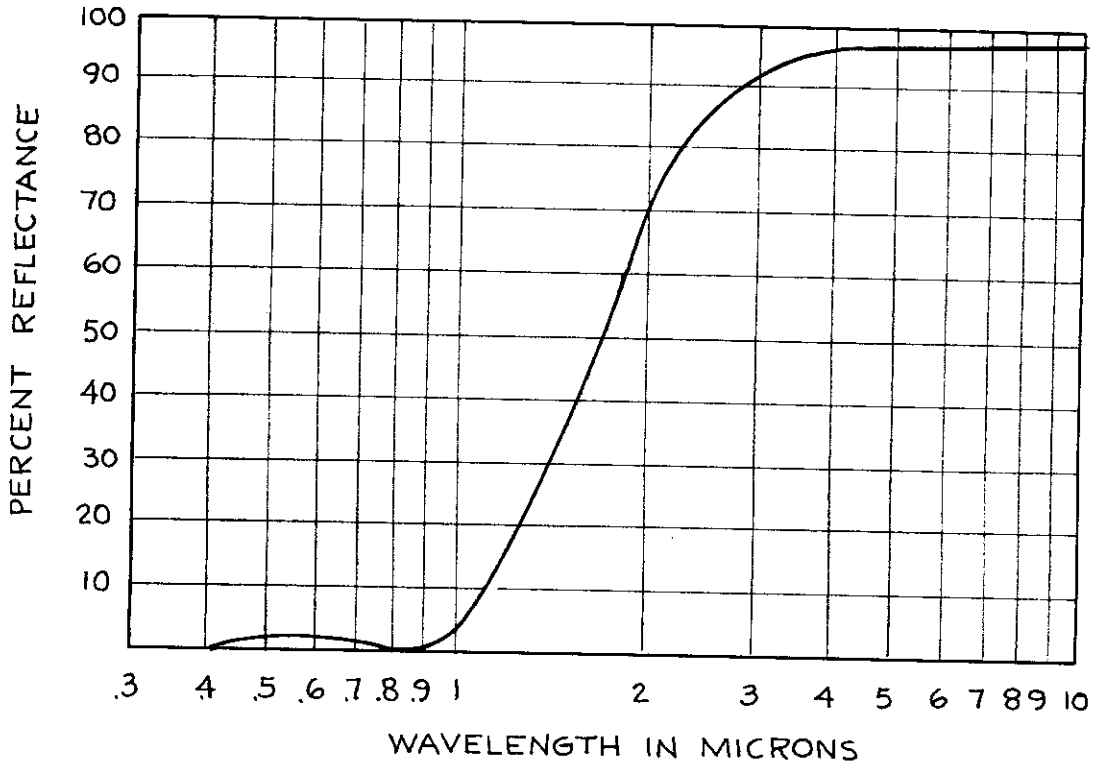

Figure 12 Theoretical Reflectivity of AL-MgF_2-AL-MgF_2